Design of Optimum Propellers

Charles N. Adkins*
Falls Church, Virginia 22042
and
Robert H. Liebeck†
Douglas Aircraft Company, Long Beach, California 90846

Improvements have been made in the equations and computational procedures for design of propellers and wind turbines of maximum efficiency. These eliminate the small angle approximation and some of the light loading approximations prevalent in the classical design theory. An iterative scheme is introduced for accurate calculation of the vortex displacement velocity and the flow angle distribution. Momentum losses due to radial flow can be estimated by either the Prandtl or Goldstein momentum loss function. The methods presented here bring into exact agreement the procedure for design and analysis. Furthermore, the exactness of this agreement makes possible an empirical verification of the Betz condition that a constant-displacement velocity across the wake provides a design of maximum propeller efficiency. A comparison with experimental results is also presented.

Nomenclature

a = axial interference factor
a' = rotational interference factor
B = number of blades
b = axial slipstream factor
C_d = blade section drag coefficient
C_l = blade section lift coefficient
C_p = power coefficient, $P/\rho n^3 D^5$
C_T = thrust coefficient, $T/\rho n^2 D^4$
C_x = torque force coefficient
C_y = thrust force coefficient
c = blade section chord
D = propeller diameter, $2R$
D' = drag force per unit radius
F = Prandtl momentum loss factor
G = circulation function
J = advance ratio, V/nD
K = Goldstein momentum loss factor
L' = lift force per unit radius
n = propeller rps
P = power into propeller
P_c = power coefficient, $2P/\rho V^3 \pi R^2$
Q = torque
R = propeller tip radius
r = radial coordinate
T = thrust
T_c = thrust coefficient, $2T/\rho V^2 \pi R^2$
V = freestream velocity
v' = vortex displacement velocity
W = local total velocity
w_n = velocity normal to the vortex sheet
w_t = tangential (swirl) velocity
x = nondimensional distance, $\Omega r/V$
α = angle of attack
β = blade twist angle
Γ = circulation
ε = drag-to-lift ratio

ζ = displacement velocity ratio, v'/V
η = propeller efficiency
λ = speed ratio, $V/\Omega R$
ξ = nondimensional radius, $r/R = \lambda x$
ξ_e = nondimensional Prandtl radius
ξ_0 = nondimensional hub radius
ρ = fluid density
σ = local solidity, $Bc/2\pi r$
ϕ = flow angle
ϕ_t = flow angle at the tip
Ω = propeller angular velocity

Superscript
$'$ = derivative with respect to r or ξ, unless otherwise noted

Introduction

IN 1936, a classic treatise on propeller theory was authored by H. Glauert.[1] In this work, a combination of momentum theory and blade element theory, when corrected for momentum loss due to radial flow, provides a good method for analysis of arbitrary designs even though contraction of the propeller wake is neglected. Although the theory is developed for low disc loading (small thrust or power per unit disc area), it works quite well for moderate loading, and in light of its simplicity, is adequate for estimating performance even for high disc loadings. The conditions under which a design would have minimum energy loss were stated by A. Betz[2] as early as 1919; however, no organized procedure for producing such a design is evident in Glauert's work. Those equations which are given by Betz make extensive use of small-angle approximations and relations applicable only to light loading conditions. Theodorsen[3] showed that the Betz condition for minimum energy loss can be applied to heavy loading as well.

In 1979, E. Larrabee[4] resurrected the design equations and presented a straightforward procedure for optimum design. However, there are still some problems: first, small angle approximations are used; second, the solution for the displacement velocity is accurate only for vanishingly small values (light loading), although an approximate correction is suggested for moderate loading; and third, there are viscous terms missing in the expressions for the induced velocities. These viscous terms must be included in the design equations if they are to be consistent with the classical propeller analysis. This approach is given later.

*Consulting Engineer. Member AIAA.
†McDonnell Douglas Fellow. Fellow AIAA.

The purpose of this article is to correct these difficulties and bring the design method into exact agreement with the analysis. It is then possible to verify empirically the optimality of the design. This work was initiated at McDonnell Douglas in 1980 in response to a requirement for simple estimates of propeller performance. In-house methods, if they existed, had been irretrievably archived. An early version was presented as AIAA Paper 83-0190. Continuous requests for copies of the paper plus some refinements to the method have motivated its publication in the Journal.

Momentum Equations

Detailed axial and general momentum theory is described by Glauert,[1] and only a brief summary is given here to emphasize several important features. Consider a fluid element of mass dm, far upstream moving toward the propeller disc in a thin, annular stream tube with velocity V. It arrives at the disc with increased velocity, $V(1 + a)$, where a is the axial interference factor. At the disc, dm exists in the annulus $2\pi r\, dr$, and the mass rate per unit radius passing through the disc is $2\pi r\rho V(1 + a)$, neglecting radial flow. The element dm moves downstream into the far wake, increasing speed to the value $V(1 + b)$, where b is the axial slipstream factor. Axial momentum theory determines b to be exactly $2a$, whereas the general theory (which includes rotation of the flow) determines b to be approximately $2a$. Using the axial approximation, which is generally accepted, the overall change in momentum of the element is $2VaF\, dm$ where F, the momentum loss factor, accounts for radial flow of the fluid. The thrust per unit radius T', acting on the annulus can now be expressed as

$$T' = \frac{dT}{dr} = 2\pi r\rho V(1 + a)(2VaF) \qquad (1a)$$

By similar arguments, the torque per unit radius Q' is given by

$$Q'/r = 2\pi r\rho V(1 + a)(2\Omega r a'F) \qquad (1b)$$

Flow geometry about a blade element at the disc is shown in Fig. 1, where W acts on the blade element with α, and acts on the disc at ϕ. F goes from about 1 at the hub (where the radial flow is typically negligible), to 0 at the tip, and is not unlike the spanwise loading of a wing. The functional form of this factor was first estimated by Prandtl[1,2] and a more accurate, though more complex, form was determined by Goldstein[5] and Lock.[6-8]

Circulation Equations

At each radial position along the blade, infinitesimal vortices are shed and move aft as a helicoidal vortex sheet. Since these vortices follow the direction of local flow, the helix angle of the spiral surface is ϕ, shown in Fig. 1. The Betz condition for minimum energy loss, neglecting contraction of the wake, requires the vortex sheet to be a regular screw surface; i.e., $r\tan\phi$ must be a constant independent of radius. Theodorsen[3]
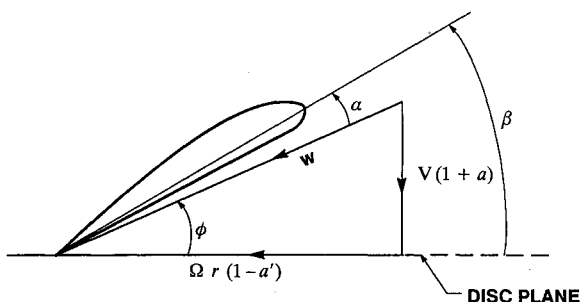

Fig. 1 Flow geometry for blade element at radial station r.
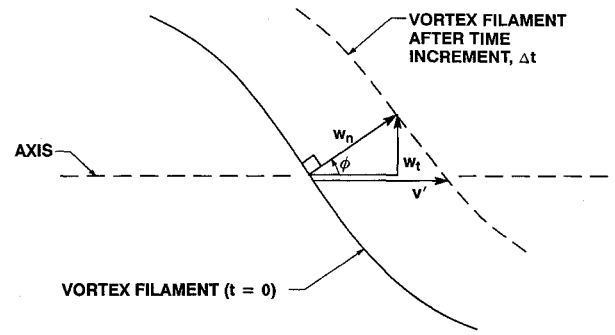

Fig. 2 Definition of displacement velocity v' in the propeller wake.

develops the Betz condition for heavy loading by including the contraction of the wake. He shows that sufficiently far downstream in the contracted wake, the vortex sheet must be the same regular screw surface for a propeller of minimum induced energy loss. This optimum vortex sheet acts as an Archimedean screw, pumping fluid aft between rigid spiral surfaces.

At the blade station, r, the total lift per unit radius is given by

$$L' = \frac{dL}{dr} = B\rho W\Gamma \qquad (2)$$

and in the wake, the circulation in the corresponding annulus is

$$B\Gamma = 2\pi r F w_t \qquad (3)$$

Setting the circulation Γ in Eq. (2) equal to that in Eq. (3) will ultimately determine that circulation distribution $\Gamma(r)$ that minimizes the induced power of the propeller.

In order to obtain $\Gamma(r)$, it is necessary to relate w_t to a more measurable quantity. Figure 2 shows the wake vortex filament at station r and the definition of the various velocity components there. The motion of the fluid must be normal to the local vortex sheet, and this normal velocity is w_n. Therefore, the tangential velocity is given by

$$W_t = w_n \sin \phi$$

However, for a coordinate system fixed to the propeller disc, the axial velocity of the vortex filament would be

$$v' = w_n/\cos \phi$$

where the increase in magnitude of v' over w_n is due to rotation of the filament. This is analogous to a barber pole where it appears that the stripes are translating in spite of the fact that only a rotational velocity exists. It will become clear that it is convenient to use v', and the corresponding displacement velocity ratio, $\zeta = v'/V$. The tangential velocity is then

$$W_t = V\zeta \sin \phi \cos \phi$$

and the circulation of Eq. (3) can be expressed as

$$\Gamma = 2\pi V^2 \zeta G/(B\Omega) \qquad (4)$$

$$G = F \times \cos \phi \sin \phi \qquad (5)$$

and x is the speed ratio given by
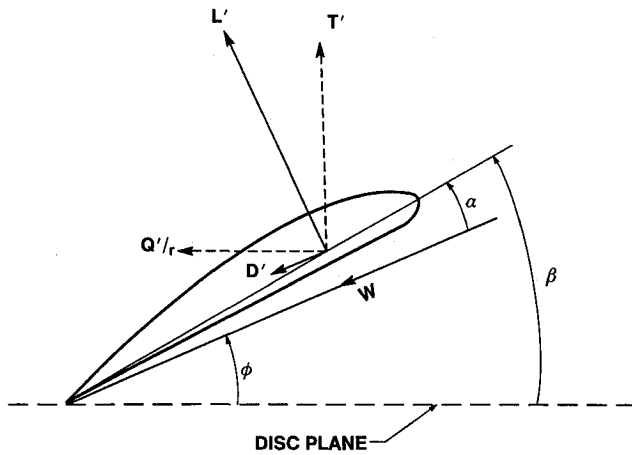
$$x = \Omega r/V$$

Fig. 3 Force diagram for a blade element.

The circulation equations for thrust T', and torque Q', per unit radius can be written by inspection of Fig. 3 as

$$T' = L' \cos \phi - D' \sin \phi = L' \cos \phi(1 - \varepsilon \tan \phi) \quad (6a)$$

$$Q'/r = L' \sin \phi + D' \cos \phi = L' \sin \phi(1 + \varepsilon/\tan \phi) \quad (6b)$$

where ε is the drag-to-lift-ratio of the blade element. Next, using Eq. (2), L' can be replaced by $\Gamma(r)$ which, in turn, is related to conditions in the wake by Eq. (3). Based on the flow in the wake, $\Gamma(r)$ is given by Eqs. (4) and (5), and T' and Q'/r are reduced to being functions of ϕ and the displacement velocity, $\zeta = v'/V$. The local flow angle ϕ will clearly be a function of the radius; however, at this stage of the analysis, the optimum distribution $\zeta(r)$ is not yet determined. Several diagrams and an excellent photograph of the vortex sheet can be found in a 1980 work by Larrabee.[9]

Condition for Minimum Energy Loss

At this point, a departure from Larrabee's[4] design procedure is made, and the momentum equations, Eqs. (1), and the circulating equations, Eqs. (6), are required to be equivalent. This condition results in the interference factors being related to ζ by the equations

$$a = (\zeta/2)\cos^2\phi(1 - \varepsilon \tan \phi) \quad (7a)$$

$$a' = (\zeta/2x)\cos \phi \sin \phi(1 + \varepsilon/\tan \phi) \quad (7b)$$

where Eqs. (4) and (5) have been used to express L' in terms of ζ, and the terms in epsilon correctly describe the viscous contribution. Equations (7), together with the geometry of Fig. 1, lead to the important simple relation

$$\tan \phi = (1 + \zeta/2)/x = (1 + \zeta/2)\lambda/\xi \quad (8)$$

Here, λ is a constant, and ξ varies from ξ_0 at the hub to unity at the edge of the disc. The relation between the two non-dimensional distances and the constant speed ratio is

$$x = \Omega r/V = (r/R)/\lambda = \xi/\lambda$$

Recalling the Betz[2] condition, $r \tan \phi = $ const, Eq. (8) proves that for the vortex sheet to be a regular screw surface, ζ must be a constant independent of radius. This is the condition for minimum energy loss. It should be noted that Eq. (8) results from Eq. (7) whether viscosity is included or not.

Constraint Equations

For design, it is necessary to specify either T, delivered by the propeller or the power P, delivered to the propeller. The nondimensional thrust and power coefficients used for design are

$$T_c = 2T/(\rho V^2 \pi R^2) \quad (9a)$$

$$P_c = 2P/(\rho V^3 \pi R^2) = 2Q\Omega/(\rho V^3 \pi R^2) \quad (9b)$$

and using these definitions, Eq. (6) can be written as

$$T'_c = I'_1\zeta - I'_2\zeta^2 \quad (10a)$$

$$P'_c = J'_1\zeta + J'_2\zeta^2 \quad (10b)$$

where the primes denote derivatives with respect to ξ, and

$$I'_1 = 4\xi G(1 - \varepsilon \tan \phi) \quad (11a)$$

$$I'_2 = \lambda(I'_1/2\xi)(1 + \varepsilon/\tan \phi)\sin \phi \cos \phi \quad (11b)$$

$$J'_1 = 4\xi G(1 + \varepsilon/\tan \phi) \quad (11c)$$

$$J'_2 = (J'_1/2)(1 - \varepsilon \tan \phi)\cos^2 \phi \quad (11d)$$

Since ζ is constant for an optimum design, a specified thrust gives the constraint equations

$$\zeta = (I_1/2I_2) - [(I_1/2I_2)^2 - T_c/I_2]^{1/2} \quad (12)$$

$$P_c = J_1\zeta + J_2\zeta^2 \quad (13)$$

Similarly, if power is specified, the constraint relations are

$$\zeta = -(J_1/2J_2) + [(J_1/2J_2)^2 + P_c/J_2]^{1/2} \quad (14)$$

$$T_c = I_1\zeta - I_2\zeta^2 \quad (15)$$

where the integration has been carried out over the region $\xi = \xi_0$ to $\xi = 1$.

Blade Geometry

For the element dr of a single blade at radial station r, let c be the chord and C_l the local lift coefficient. Then, the lift per unit radius of one blade is

$$\rho W^2 c C_l/2 = \rho W \Gamma$$

where Γ is given by Eq. (4). It follows directly that

$$Wc = 4\pi\lambda GVR\zeta/(C_l B) \quad (16)$$

Assume for the moment that ζ is known; then the local value of ϕ is known from Eq. (8), and the above relation is a function only of the local lift coefficient. Since the local Reynolds number is Wc divided by the kinematic viscosity, Eq. (16) plus a choice for C_l will determine the Reynolds number and ε, from the airfoil section data. The total velocity is then determined by Fig. 1 as

$$W = V(1 + a)/\sin \phi \quad (17)$$

where a is given by Eq. (7), and the chord is then known from Eq. (16). If the choice for C_l causes ε to be a minimum, then viscous as well as momentum losses will in most cases be minimized, and overall propeller efficiency will be the highest possible value. For preliminary considerations, it is usually sufficient to choose one C_l, the design C_l, for determining blade geometry. (Any C_l specification is permissible as long as the optimum blade loading distribution, $cC_l(r)$, is maintained.) Since α is known from C_l and Reynolds number, the blade twist with respect to the disc is $\beta = \alpha + \phi$. G is zero

at the edge of the disc, and the tip chord is therefore always zero for a finite lift coefficient.

Design Procedure

Either F or K, relation for the momentum loss function can be selected. For the sake of simplicity, only the Prandtl relation is described as

$$F = (2/\pi)\text{arc } \cos(e^{-f}) \tag{18}$$

where

$$f = (B/2)(1 - \xi)/\sin \phi_t \tag{19}$$

and ϕ_t is the flow angle at the tip. From Eq. (8)

$$\tan \phi_t = \lambda(1 + \zeta/2) \tag{20}$$

so that a choice for ζ determines the function F as well as ϕ by

$$\tan \phi = (\tan \phi_t)/\xi \tag{21}$$

which is simply the condition that the vortex sheet in the wake is a rigid screw surface ($r \tan \phi = \text{const}$). For an initial value, $\zeta = 0$ will suffice.

The design is initiated with the specified conditions of power (or thrust), hub and tip radius, rotational rate, freestream velocity, number of blades, and a finite number of stations at which blade geometry is to be determined. Also, the design lift coefficient—one for each station if it is not constant—must be specified. The design then proceeds in the following steps:

1) Select an initial estimate for ζ ($\zeta = 0$ will work).

2) Determine the values for F and ϕ at each blade station by Eqs. (18–21).

3) Determine the product Wc, and Reynolds number from Eq. (16).

4) Determine ε and α from airfoil section data.

5) If ε is to be minimized, change C_l and repeat Steps 3 and 4 until this is accomplished at each station.

6) Determine a and a' from Eq. (7), and W from Eq. (17).

7) Compute the chord from step 3, and the blade twist $\beta = \alpha + \phi$.

8) Determine the four derivatives in I and J from Eq. (11) and numerically integrate these from $\xi = \xi_0$ to $\xi = 1$.

9) Determine ζ and P_c from Eqs. (12) and (13), or ζ and T_c from Eqs. (14) and (15).

10) If this new value for ζ is not sufficiently close to the old one (e.g., within 0.1%) start over at step 2 using the new ζ.

11) Determine propeller efficiency as T_c/P_c, and other features such as solidity.

The above steps converge rapidly, seldom taking more than three or four cycles. An accurate description of viscous losses can be obtained by creating another design with ε equal to zero and noting the difference in propeller efficiency.

Analysis of Arbitrary Designs

The analysis method is outlined here in order to discuss problems of convergence for off design and for square-tipped propellers in general, and to point out two minor errors in Glauert's work. Figure 4, which is simply an alternate version of Fig. 3, shows the relation between the propeller force coefficients, C_y and C_x, and the airfoil coefficients, C_l and C_d. The equations are

$$C_y = C_l \cos \phi - C_d \sin \phi = C_l(\cos \phi - \varepsilon \sin \phi)$$

$$C_x = C_l \sin \phi + C_d \cos \phi = C_l(\sin \phi + \varepsilon \cos \phi)$$
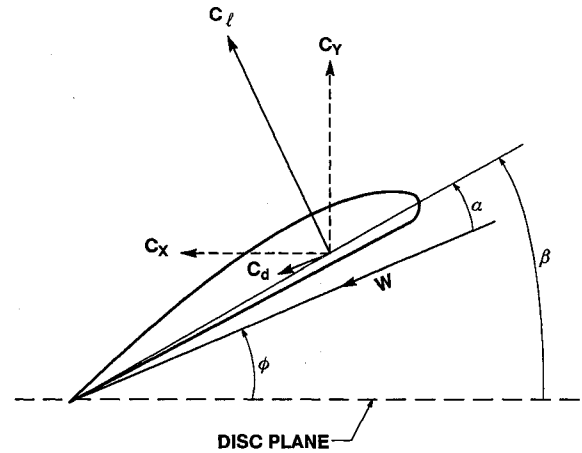

Fig. 4 Force coefficients for propeller blade element analysis.

and the relations for the thrust T' and torque Q' per unit radius are then

$$T' = (\tfrac{1}{2})\rho W^2 Bc C_y \tag{22a}$$

$$Q'/r = (\tfrac{1}{2})\rho W^2 Bc C_x \tag{22b}$$

Again, it is required that the loading Eqs. (22) be exactly equal to the momentum result Eqs. (1). With the use of the flow geometry in Fig. 1, this requires the interference factors to be

$$a = \sigma K/(F - \sigma K) \tag{23a}$$

$$a' = \sigma K'/(F + \sigma K') \tag{23b}$$

where

$$K = C_y/(4 \sin^2 \phi) \tag{24a}$$

$$K' = C_x/(4 \cos \phi \sin \phi) \tag{24b}$$

and σ is given by

$$\sigma = Bc/(2\pi r)$$

Equations (23) correct the placement of the factor F used by Glauert in his equations (5.5) of Chapter VII as identified by Larrabee.[4]

The relation for the flow angle is obtained from Fig. 1 and Eqs. (23) as

$$\tan \phi = [V(1 + a)]/[\Omega r(1 - a')] \tag{25}$$

For determining the function, F, in Eq. (18), Glauert suggests the relation $\sin \phi_t = \xi \sin \phi$ be used in Eq. (19). It is recommended that Eq. (21) be used instead, i.e.,

$$\tan \phi_t = \xi \tan \phi$$

which is exact for the analysis of an optimally designed propeller at the design point.

The analysis procedure requires an iterative solution for the flow angle ϕ at each radial position, ξ. An initial estimate for ϕ can be obtained from Eq. (8) by setting ζ equal to zero. Since β is known, the value for α in Fig. 3 is $\beta - \phi$, and the airfoil coefficients are known from the section data. The Reynolds number is determined from the known chord and W, which is obtained from Fig. 1 and Eq. (23a), and the new estimate for ϕ is then found from Eq. (25). A direct substitution of the new ϕ for the old value will cause adequate convergence for an optimum design which is being analyzed at the design point. However, for analysis off-design and for

nonoptimum designs, some recursive combination of the old and new values for ϕ is required to cause adequate convergence. Under some conditions (usually near the tip), convergence may not be possible at all due to large values for the interference factors, a and a', in Eq. (23). Since F is zero at the tip and σ is not for a square tip propeller, the value for a is -1 and a' is $+1$. Such values are physically impossible since the slipstream factors are approximately twice the values at the rotor plane. Wilson and Lissaman[10] suggest empirical relations for resolving this problem, whereas Viterna and Janetzke[11] give empirical arguments for clipping the magnitude of a and a' at the value 0.7 (σ/F at the tip is finite at the design point for an optimum propeller).

For analysis, the conventional thrust and power coefficients are

$$C_T = T/(\rho n^2 D^4)$$

$$C_p = P/(\rho n^3 D^5)$$

Using Eqs. (22) and (24), the differential forms with respect to ξ are given by

$$C_T' = (\pi^3/4)\sigma C_y \xi F^{32}/[(F + \sigma K')\cos \phi]^2$$

$$C_p' = C_T' \pi \xi C_x/C_y$$

When these have been integrated from the hub to the tip, the propeller efficiency is

$$\eta = C_T J/C_p$$

where $J = V/(nD)$ is the advance ratio. Propeller performance is typically described by plots of C_T, C_p, and η vs J.

Airfoil Section Data

The proper accounting for blade section (airfoil) characteristics has proven essential for accurate and reliable esti-

Fig. 5 Example of airfoil section characteristics including normal and chord force coefficients.

mation of propeller performance, and the extent of airfoil data required for propeller analysis exceeds that which is typically used in analysis of wings. Between takeoff, climb, and cruise, propellers typically operate over a relatively wide range of blade section Reynolds numbers—a variation by factor of 5 is not uncommon. Also, during takeoff, climb, and windmilling, some portion of a propeller blade is likely to be stalled, either positively or negatively. An example set of characteristics for the NACA 4415 airfoil is given in Fig. 5. These would be supplemented by additional drag data in the unstalled region for a range of Reynolds numbers.

Empirical Optimality

In Chapter VII of Glauert's work, his equation (2.20) shows that when blade friction is neglected, the most favorable distribution of circulation is where the displacement velocity is constant across the wake. Here, the term $x^2/(1 + x^2)$ is the small-angle approximation of G, given by Eq. (5) in this article. The effect of profile drag is shown by Glauert in his equation (3.5), which states that the optimum distribution for the displacement velocity ratio is

$$\zeta = \zeta_0 - \varepsilon X \tag{26}$$

where the effect of profile drag on thrust has been ignored. In order to study this problem empirically, consider a general function $H(x)$ and the two first-order terms of its Laurent series, $1/x$ and x, and describe the displacement velocity distribution as

$$\zeta = \zeta_0 + \delta_1 x + \delta_2/x \tag{27}$$

which includes the case of Eq. (26). It is desired to find values for δ_1 and δ_2 which maximize propeller efficiency subject to the constraints of Eqs. (10). To solve this problem, ζ in Eqs. (10) is replaced by Eq. (27). Then, a choice for δ_1 and δ_2 will enable a determination of ζ_0 and a calculation of overall propeller efficiency. A systematic study of various propeller conditions was undertaken using the design and analysis procedures of this article. Nonzero values for δ_1 and δ_2 that caused an increase in propeller efficiency could not be found under any conditions. Therefore, it was concluded that a constant displacement velocity is at least locally optimum whether profile drag is considered or not. Momentum and viscous losses are then uncoupled; former is minimized by constant displacement velocity, the latter by choosing a C_l distribution so that the drag-to-lift ratio is a minimum everywhere.

Some may criticize the authors for including viscous terms in the development of the optimized circulation distribution for the propeller design problem. Certainly, this is contrary to classical lifting-line wing theory where the analogous elliptic lift distribution is obtained inviscidly. However, it has been shown that the combined momentum-circulation equations, Eqs. (7), produce the screw surface equations, Eqs. (8), whether viscosity is included or not. It is evident in Eq. (11) that the momentum and viscous terms are directly separable for use in Eq. (10). The viscous terms, when integrated in Eq. (10), account for the difference in power and thrust between an inviscid and viscous propeller design. If one accepts the classical blade element analysis equations as a measure of performance, the momentum and viscous losses are indeed uncoupled, and the viscous design equations produce a propeller with minimal losses.

Alternatively, if one is still concerned about including viscosity in the design procedure, a propeller could be designed inviscidly and the blade section drag simply added to the inviscid design. This would require that the analysis procedure be applied with drag set equal to zero when solving for the induction velocities. The performance of the propeller would then be obtained by adding drag to this inviscid solution without altering the induction velocities. However, this would
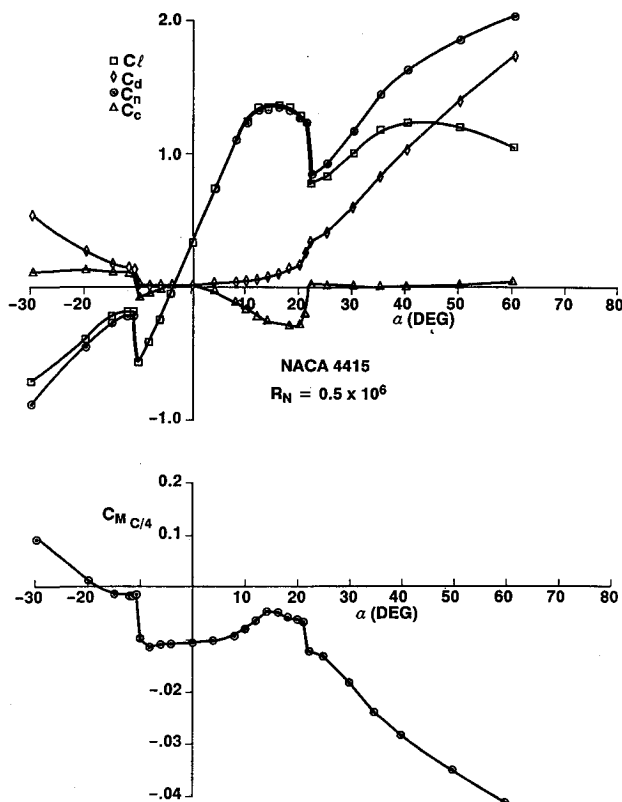
Table 1 Propeller design solution

r	c	β	φ	RN	a	a'
0.5000	0.3424	58.3125	54.8118	0.4449	0.0348	0.0633
0.8958	0.4605	41.8645	38.3637	0.8104	0.0644	0.0365
1.2917	0.4269	32.2669	28.7661	0.9834	0.0804	0.0219
1.6875	0.3569	22.2978	22.7927	1.0295	0.0890	0.0142
2.0833	0.2796	18.7971	18.7971	0.9740	0.0938	0.0098
2.4792	0.1913	15.9619	15.9619	0.7830	0.0968	0.0072
2.8750	0.0000	13.8552	13.3552	0.0000	0.0000	0.0000

Input: brake horsepower = 70, 2 blades; hub diam = 1 ft, tip diam = 5.75 ft; blade section: NACA 4415, C_l = 0.7, velocity = 110 mph, rpm = 24001.
Output: thrust = 207.61 lb, η = 0.86996.
Note: a and a' have been set equal to zero at the tip.

Table 2 Propeller analysis solution

r	φ	C_l	RN	a	a'
0.5000	54.8116	0.7000	0.4449	0.0348	0.0633
0.8958	38.3638	0.7000	0.8104	0.0644	0.0365
1.2917	28.7661	0.7000	0.9834	0.0804	0.0219
1.6875	22.7927	0.7000	1.0295	0.0890	0.0142
2.0833	18.7971	0.7000	0.9740	0.0938	0.0098
2.4792	15.9619	0.7000	0.7830	0.0968	0.0072
2.8750	12.5862	0.7000	0.0000	0.0000	0.0000

Input: propeller geometry from Table 1; r, C, and β at the same radial locations; velocity = 110 mph, rpm = 2400.
Output: brake horsepower = 70, thrust = 207.61 lb, η = 0.86996.
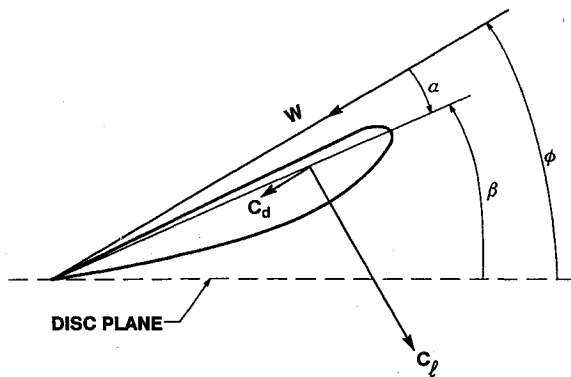

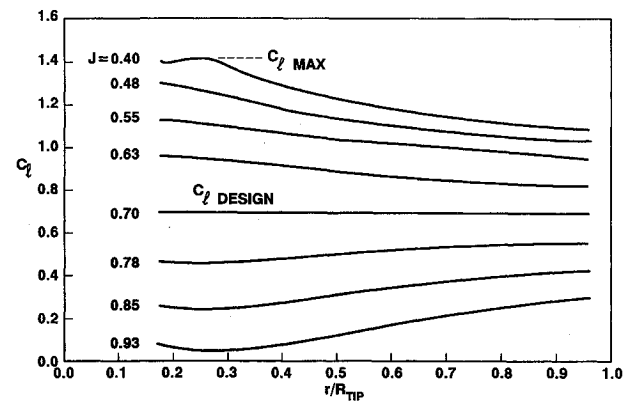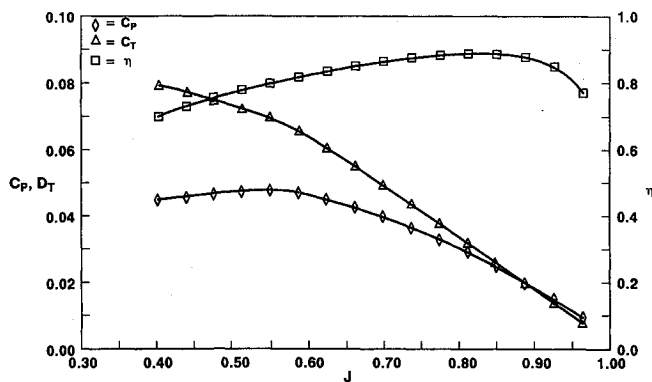Fig. 6 Force coefficients for windmill blade element.

Fig. 8 C_l distributions for example propeller.

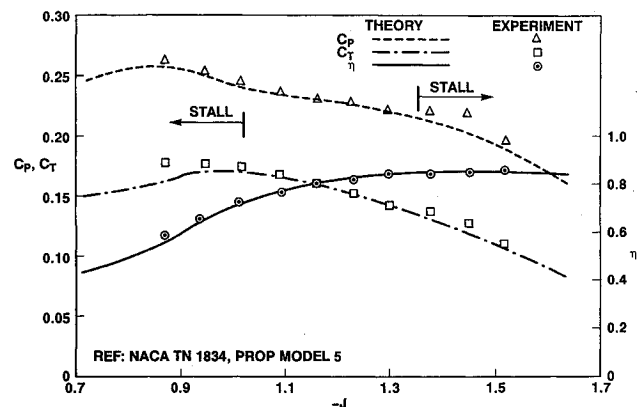Fig. 7 Example of propeller performance.

Fig. 9 Comparison of theory and experiment.

require an additional layer of iteration to achieve a specified design thrust or power. In light of the favorable agreement between the present theory and the experimental results given later in this article, it is argued that such an increase in complexity is not justified.

Windmills

All of the analyses described in this article are directly applicable to the windmill problem after a minor adjustment in the angle definitions of Fig. 1. The corresponding flow

geometry for a windmill is shown in Fig. 6, where the primary distinction is that the blade section is inverted (as compared with a propeller), and the local angle of attack is measured from below the local velocity vector. Corresponding relations for the angles are

$$\text{windmill} \quad \alpha = \phi - \beta$$

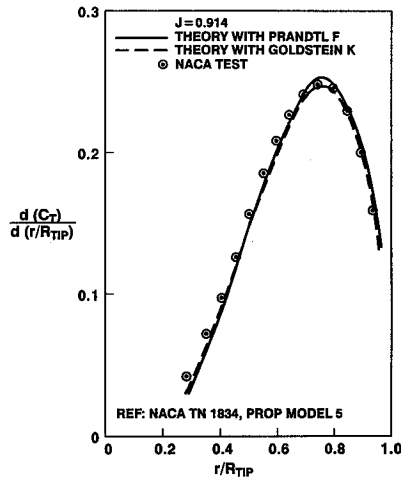$$\text{propeller} \quad \alpha = \beta - \phi$$

Fig. 10 Comparison of propeller analyses thrust coefficient.

as shown in Figs. 6 and 1, respectively. In these figures, C_l for the windmill is negative with respect to that for the propeller, and this sign change together with the angle definition will convert the propeller methods to the windmill application. For the design case, the input P_c value should be negative, and the resulting values of v' (and the interference factors a and a') and T_c will also be negative. (Thrust is of less interest for a windmill since it typically represents the tower load and is not a main performance parameter.) Similarly, the analysis results for a windmill rotor will yield negative values for both P_c and T_c.

Examples

As a sample calculation, the design of a propeller for a light airplane is considered. The design conditions and the resulting design are described in Table 1 which gives for each radial station: blade chord, blade pitch angle, local flow angle, local Reynolds number, and the interference coefficients a and a'.

This propeller geometry has, in turn, been analyzed at the design condition and the result is given in Table 2. Agreement is virtually exact. Analysis over a range of values of the advance ratio, $J = V/(nD)$, provides the typical propeller performance plots which are shown in Fig. 7, and Fig. 8 gives the blade lift coefficient distribution over a range of Js where the design condition is the $C_l = 0.7$ and is a constant line at $J = 0.7$.

A calibration of the method is given by comparing its theoretical prediction with experimental results. Reid[12] has evaluated several conventional propellers extensively by experiment, and one of these has been chosen for comparison. Figure 9 gives C_p, C_T, and η vs J for both Reid's experiments and the corresponding theoretical prediction. The agreement here is quite good, with most of the disparity occurring after the blade is stalled. This propeller uses NACA 16-series airfoils, and no poststall data were available.

Figure 10 gives the comparison of the blade thrust coefficient distribution as measured by Reid and calculated by the method. Two theoretical results are shown: one using F, and the other using the more complex (from a calculation point of view) K. In principle, the accuracy of the method should be better with the Goldstein factor for a propeller with few blades—this example had three blades—and the two factors should give similar results as the number of blades is increased. The results of Fig. 10 confirm this trend, and the overall comparison for both factors is regarded as quite good.

Conclusions and Recommendations

The propeller theory of Glauert has been extended to improve the design of optimal propellers and refine the calculation of the performance of arbitrary propellers. Extensions of the theory include 1) elimination of the small angle assumptions in the optimal design theory; 2) accurate calculation of the vortex displacement velocity which properly accounts for the blade section drag; and 3) elimination of the small angle assumptions in the Prandtl momentum loss function for both design and analysis. These extensions bring the design and analysis procedures to exact numerical agreement within the precision of computer analysis. The primary approximation remaining in both procedures is the use of the axial momentum equations which require the increase in wake velocities to be twice those at the disc. Under certain conditions this approximation is not good and gives rise to the unnatural conditions and convergence problems described in the analysis section. Improvements might be made by replacing the axial momentum equations with relations more closely aligned with the general theory, particularly in those differential stream tubes in which "heavy loading" exists. Such conditions appear to be more prevalent in the analyses at off-design conditions than in the design itself, and, when combined with poststall misknowledge, can lead to large errors in analysis. However, for design and analysis within the conventional operating regime, both procedures are simple, accurate, and reliable. This method has been extended by Page and Liebeck[13] to the design and analysis of dual-rotation propellers. A favorable comparison between theory and experiment was also observed.

References

[1]Glauert, H., "Airplane Propellers," *Aerodynamic Theory*, edited by W. Durand, Div. L, Vol. 5, Peter Smith, Gloucester, MA, 1976, pp. 169–269.

[2]Betz, A., with appendix by Prandtl, L., "Screw Propellers with Minimum Energy Loss," Gottingen Reports, 1919, pp. 193–213.

[3]Theodorsen, T., *Theory of Propellers*, McGraw-Hill, New York, 1948.

[4]Larrabee, E., "Practical Design of Minimum Induced Loss Propellers," Society of Automotive Engineers, Business Aircraft Meeting and Exposition, Wichita, KS, April 1979.

[5]Goldstein, S., "On the Vortex Theory of Screw Propellers," *Proceedings of the Royal Society of London, Series A*, Vol. 123, 1929, pp. 440–465.

[6]Lock, C., "The Application of Goldstein's Airscrew Theory to Design," British Aeronautical Research Committee, RM 1377, Nov. 1930.

[7]Lock, C., "An Application of Prandtl's Theory to an Airscrew," British Aeronautical Research Committee, RM 1521, Aug. 1932.

[8]Lock, C., "Tables for Use in an Empirical Method of Airscrew Strip Theory Calculations," British Aeronautical Research Committee, RM 1674, Oct. 1934.

[9]Larrabee, E., "The Screw Propeller," *Scientific American*, Vol. 243, No. 1, 1980, pp. 134–148.

[10]Wilson, R., and Lissaman, P., "Applied Aerodynamics of Wind Power Machines," Oregon State Univ., NSF/RA/N-74-113, PB-2318595/3, Corvallis, OR, July 1974.

[11]Viterna, A., and Janetzke, D., "Theoretical and Experimental Power from Large Horizontal-Axis Wind Turbines," *Proceedings from the Large Horizontal-Axis Wind Turbine Conference*, DOE/NASA-LeRC, July 1981.

[12]Reid, E. G., "The Influence of Blade-Width Distribution on Propeller Characteristics," NACA TN 1834, March 1949.

[13]Page, G. S., and Liebeck, R. H., "Analysis of Dual-Rotation Propellers," AIAA Paper 89-2216, Aug. 1989.